Available online at www.sciencedirect.com
SCIENCE DIRECT®
International Journal of Solids and Structures 42 (2005) 503–515
INTERNATIONAL JOURNAL OF SOLIDS and STRUCTURES
www.elsevier.com/locate/ijsolstr

Homogeneity of isostatic pressure-assisted sintering of agglomerated powder

Andrey Maximenko, Eugene Olevsky *

Department of Mechanical Engineering, San Diego State University, 5500 Campanile Dr., San Diego, CA 92182-1323, USA

Received 19 May 2004
Available online 14 August 2004

Abstract

This article is dedicated to the modeling of the pressure-assisted sintering of agglomerated powders by the grain-boundary and the surface diffusion transport. Agglomerates are treated as volumes with dense particle packing. Kinetics of sintering during consolidation is estimated by a direct numerical analysis of the matter redistribution by diffusion around a single neck between identical spherical particles. Type of packing is introduced into the model through the definition of the packing angle and a special symmetry boundary condition for diffusion fluxes. The numerical analysis of sintering parameters for a single neck allows the evaluation of macroscopic viscosities of the material for different types of the particle packing and enables the estimation of the densification rate of agglomerates and non-agglomerated elements of powder compacts. Calculations show that, despite low initial density and low initial viscosity of a loose powder around agglomerates, isostatic pressing cannot provide a complete equalization of local densities in an agglomerated powder. In all considered cases, agglomerates have reached final density faster than elements with looser packing.

Keywords: Sintering; Agglomeration; Particle packing; Densification

1. Introduction

An internal packing structure of particles in a powder body is, as a rule, inhomogeneous at the scale level comparable to the particle size. This structural level is usually identified as ''mesoscopic'' to distinguish it from the macroscopic level of a powder body as a whole and from the microscopic atomic level. The

* Corresponding author. Tel.: +1 619 594 6329; fax: +1 619 594 3599.
E-mail address: olevsky@engineering.sdsu.edu (E. Olevsky).

0020-7683/$ - see front matter © 2004 Elsevier Ltd. All rights reserved.
doi:10.1016/j.ijsolstr.2004.06.040

average density of powder compacts is a mean value over all density variations in mesoscopic volumes of a powder body. Mesoscopic volumes with high packing density are identified as ''agglomerates''. Agglomerates are separated from each other by volumes of lower packing densities. An important feature of a powder body is associated with the fact that mesoscopic density variations are not small. They are comparable with the average density. As a result, a powder body at the mesoscopic level can be considered as a mixture of different phases with different densities, even if it consists of identical particles (due to their spatially non-uniform packing). This specific feature of powder bodies sometimes reveals itself during powder consolidation. For example, agglomerates lead to the crack development during sintering due to differential shrinkage rates in volumes with different packing densities (Lange, 1989).

The physical origins of agglomerates can be different. In most cases, their development is a result of the history of powder processing or high activity of interparticle attraction forces like Van-Der-Waals forces or capillary forces in wet processing. Formation of agglomerates is typical for fine powders, especially for nano-powders (Mayo, 1995) since all interparticle attraction forces are inversely proportional to the particle size. Details of mesoscopic variations of powder packing structures are difficult to determine by experimental analyses. This is why they are rarely used in the macroscopic modeling of consolidation processes. However, the analysis of the evolution of mesoscopic variations in powder materials is vital for the optimization of the grain size distribution in powder compacts after sintering. During sintering, agglomerates are densified faster than a powder body as a whole. As a result, a heavy grain growth is observed in agglomerated volumes, since the grain growth rate is directly related to density (Rahaman, 1995). In pressureless sintering it is difficult to obtain the grain size less than the agglomerate size (Mayo, 1995). This situation is impractical for the production of nanostructured materials since their unique properties depend on the uniformity of fine grain structures. Therefore, a successful consolidation method should reduce mesoscopic differences in materials to provide a uniform grain growth.

The present article is dedicated to the analysis of the isostatic pressure-assisted sintering of an agglomerated powder. All particles are assumed to be identical spheres. Mesoscopic differences appear due to the variations of the particle coordination numbers throughout a powder volume. The coordination number of a particle is the number of its neighbor particles. In agglomerates the coordination number is high and it is lower for a loose powder between agglomerates.

2. Modeling of a single inter-particle neck behavior during pressure-assisted sintering

In the present modeling approach the grain-boundary and the surface diffusions are the main mechanisms of the matter redistribution. This is the case for the sintering of fine and nano- powders (Rahaman, 1995). Geometrical assumptions used for the modeling of the inter-particle neck growth during pressure-assisted sintering are shown in Fig. 1. The interaction between necks during densification is considered in a simplified homogenized manner. The influence of neighbor necks is treated as the influence of a uniform band of contacts around the equator of two particles forming the neck (Bouvard and McMeeking, 1996). As a result, the problem of the neck interaction during sintering becomes axisymmetrical. All necks are assumed to be the same during isostatic pressure-assisted sintering. From the symmetry considerations it is clear that the middle line at the particle surface between different necks is the line of zero matter transport across it. Position of this line depends on the coordination number of the powder packing and in an axisymmetrical statement of the problem it is simply a circle corresponding to some packing angle φ (see Fig. 1). For a simple cubic packing, the packing angle is $\varphi = \pi/4$ and the coordination number of the packing is $Z = 6$. In the case of a face-centered cubic packing of particles, the coordination number is $Z = 12$, and due to the existence of four close-packed planes (Allen and Thomas, 1999), the packing angle can be taken equal to $\varphi = \pi/6$. In numerical modeling of diffusion processes it is sufficient to consider only the matter transport at the part of the particle surface within the spherical

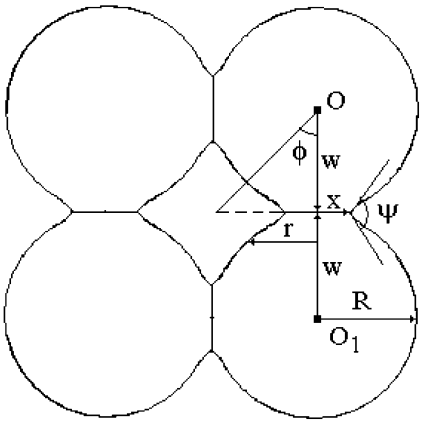

Fig. 1. Schematics of the geometry of particle packing.

angle corresponding to the packing angle φ with the zero-flux boundary condition at the above-mentioned middle line. This line is a circular intersection of the boundary of the spherical angle with the particle surface.

The internal structure of a powder compact has been modeled as a mixture of high-density agglomerates with an f.c.c. particle packing and a loose powder in simple cubic packing. In the framework of our assumptions the modeling of the neck growth for different types of packing is reduced to the analysis of the influence of the packing angle φ on diffusion processes. The model describes the consolidation processes only for the first stage of sintering with porosity higher than 0.1–0.15 when single necks between particles are discernible (Rahaman, 1995). At the second stage, closed porosity is predominant in a powder body and the considered neck geometry is not applicable anymore. However, the results of the modeling for small porosities and large neck radii correspond to the two-dimensional plane problem of the sintering of infinitely long wires with round cross-sections (Maximenko et al., 2002). That is why we have modeled the neck development for the entire range of porosity values.

The formulation of the boundary-value problem for the modeling of the diffusion matter redistribution during pressure-assisted sintering of identical particles is well established (Bouvard and McMeeking, 1996; Allen and Thomas, 1999). The grain-boundary matter flux at the edge of an axisymmetrical circular neck is given by the equation

$$J_{\mathrm{r}} = \frac{4D_{\mathrm{g}}\delta_{\mathrm{g}}\Omega\gamma_{\mathrm{s}}}{RxkT}\left(RK(x) + 2\frac{R}{x}\sin\left(\frac{\psi}{2}\right) - \bar{\sigma}\right) \tag{1}$$

where J_{r} is the material volume passing out of the grain-boundary, x is the neck radius, R is the particle radius, D_{g} is the grain-boundary diffusivity, δ_{g} is the grain-boundary thickness, Ω is the atomic volume, k is the Boltzmann's constant, T is the absolute temperature, γ_{s} is the specific surface energy, $K(x)$ is the sum of the principal curvatures at the edge of the neck, ψ is the dihedral angle, σ is the average normal component of external stress at the neck and $\bar{\sigma}$ stands for the dimensionless combination $\sigma R/\gamma_{\mathrm{s}}$.

Note that σ is not a macroscopic stress in the material. It is the result of the macroscopic stress concentration at neck surfaces. For an isostatic loading, the stress σ can be calculated simply as $\sigma = pR^2/Zx^2$, where p is the external pressure. In the calculations of $K(x)$ the curvature is defined to be positive if the center of curvature is outside of a particle. The shrinkage rate can be found through J_{r} as

$$\dot{w} = -\frac{J_{\mathrm{r}}}{x}$$

where $2\dot{w}$ is the rate of the approach of one particle towards another and dot above w denotes the derivative with respect to time.

The diffusion flux J_s along free surfaces of particles is a function of gradients of the surface curvature:

$$J_s = -\frac{\delta_s D_s \Omega \gamma_s}{kT} \frac{dK}{ds} \tag{2}$$

where δ_s is the thickness of the surface layer in which diffusion takes place, D_s is the surface diffusivity, and s is a curvilinear coordinate along the surface. The surface flux leads to the deposition of the material with the displacement rate v normal to the surface and equal to

$$v = \frac{1}{r} \frac{d(rJ_s)}{ds} \tag{3}$$

where r is the distance from the centerline of the particles to the considered element of the surface. The condition of the flux continuity at the edge of the neck gives:

$$J_r = 2J_s \tag{4}$$

Eqs. (1) and (4) provide the boundary conditions for the problem of the matter redistribution by the surface diffusion. The physical time can be normalized as the characteristic time τ_s of the surface diffusion kinetics:

$$\tau_s = \frac{kTR^4}{\delta_s D_s \Omega \gamma_s} \tag{5}$$

The relative rate of the grain boundary and the surface diffusions has been estimated through the following parameter:

$$\xi = \frac{\delta_g D_g}{\delta_s D_s} \tag{6}$$

The parameter ξ is an indicator of the process non-equilibrium. If the parameter ξ is small ($\xi \leqslant 0.01$), the rapid matter redistribution by the surface diffusion keeps free surfaces of particles close to their equilibrium positions during the entire sintering process. For larger ξ values, the matter redistribution is substantially non-equilibrium. In general, the full spectrum of sintering conditions in the present model can be described through variations of the four independent parameters: ξ, $\bar{\sigma}$, ψ, φ. The dihedral angle ψ has been taken to be constant ($\psi = 0.8\pi$) in all the calculations. This value lies within the typical range for ceramic materials (Hague and Mayo, 1999). The special role in the present modeling belongs to the analysis of the influence of variations of the packing angle φ on the densification homogeneity.

The numerical approach is based on the method of lines (Maximenko et al., 2002) where all the derivatives along the surfaces in Eq. (2) for matter fluxes are replaced by their finite-difference approximations. An implicit numerical scheme has been used for the approximation of the time derivatives. The details of the numerical approach can be found in (Maximenko et al., 2002). The numerical calculations allow the prediction of the evolutions of the distances between particles, neck radii and particle shapes for different φ, ξ, $\bar{\sigma}$.

In order to allow the comparison with the results of other publications, three types of functions have been obtained and analytically approximated based on the numerical modeling: the shrinkage rate as a function of the neck radius, the viscosity of the neck as a function of the neck radius, and the neck radius as a function of porosity. The shrinkage rate $\dot{w}\tau_s/R$ for a single contact between two particles as a function of the neck radius has been obtained in (Bouvard and McMeeking, 1996) in the form

$$\frac{\dot{w}\tau_s}{R\xi} = -\frac{\alpha(\xi)}{(x/R)^4} + \frac{\beta(\xi)\bar{\sigma}}{(x/R)^2} \tag{7}$$

where $\alpha(\xi)$, $\beta(\xi)$ are some functions of ξ. It has been found in (Bouvard and McMeeking, 1996) that $\beta(\xi)\approx 4$. The first term in (7) describes the shrinkage rate during free sintering and the second term is a contribution of an external loading. In order to obtain an approximation similar to (7) for our numerical results, the least-square method has been applied for the approximation of the logarithm of the shrinkage rate by a combination of the four basic functions: 1, x/R, $\ln(x/R)$, $\ln(\frac{x_{\max}-x}{R})$, where $x_{\max}$ is the maximum attainable neck radius. The value of $x_{\max}$ depends on the packing angle φ. It is equal to 0.84 for $\varphi=\pi/4$ and 0.54 for $\varphi=\pi/6$. The results of the numerical prediction for the free sintering shrinkage rates for different packing angles and their approximations are shown in Fig. 2. In the analytical form, for $\xi=0.1$ they are:

$$\begin{aligned}\frac{\dot{w}\tau_s}{R} &= \exp(0.16-5.8x/R)\frac{1}{(x/R)^{3.55}(0.84-x/R)^{2.09}} \quad \text{for } \varphi=\pi/4\\ \frac{\dot{w}\tau_s}{R} &= \exp(0.20-9.4x/R)\frac{1}{(x/R)^{3.4}(0.54-x/R)^{1.79}} \quad \text{for } \varphi=\pi/6\end{aligned} \tag{8}$$

The clear difference between (8) and (7) is in the fact that our results demonstrate an exponential decay of the free sintering shrinkage rates with the increase of the neck radius. In general, relationships (8) indicate which terms are necessary for the precise assessment of the shrinkage rate. Simpler approximations are impossible without a substantial loss of accuracy. Results of the approximations (8) are given as dotted lines in Fig. 2.

Relationship (7) can be rewritten as

$$\dot{\varepsilon}=\dot{\varepsilon}_f+\frac{\bar{\sigma}}{\eta} \tag{9}$$

where $\dot{\varepsilon}$, $\dot{\varepsilon}_f$ stand for the total shrinkage rate and the free shrinkage rate, respectively. Coefficient η is termed "neck viscosity". The numerical data for the neck viscosity as a function of the neck radius are given

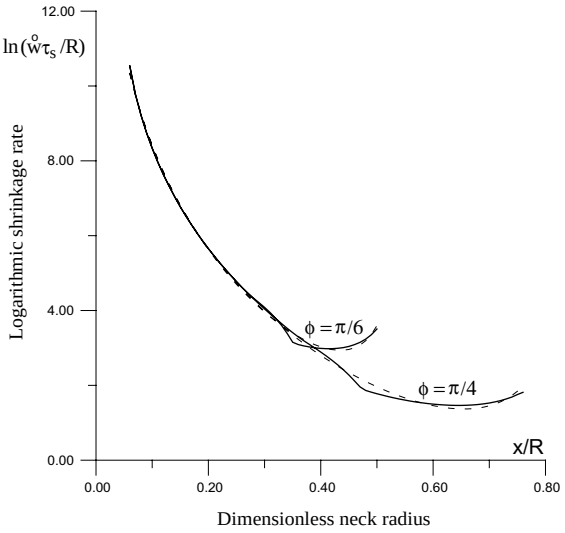

Fig. 2. Shrinkage rate of free sintering as a function of the neck radius. The dotted lines show results of approximations (8).

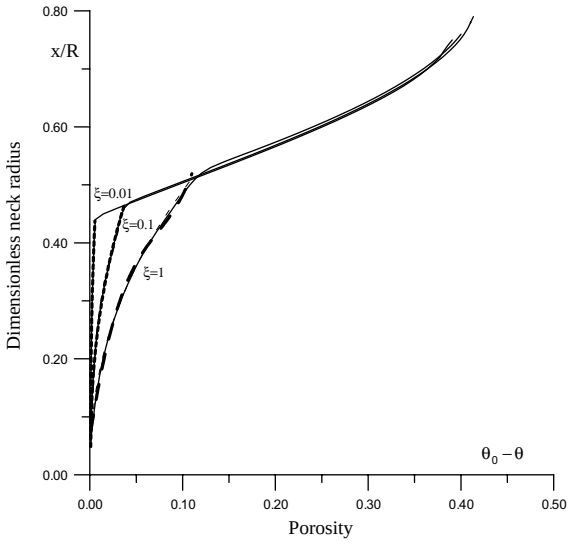

Fig. 3. Dimensionless neck radius as a function of porosity for different ξ and $\varphi = \pi/4$.

elsewhere (Maximenko and Olevsky, 2004). It is shown that the products $\eta\xi$ are close to each other for all ξ. For $\xi = 0.1$, the approximation gives

$$\eta = 2.6(x/R)^2 \tag{10}$$

The comparison between (10) and (7) indicates that our results for the neck viscosity are practically identical to the results of Bouvard and McMeeking (1996). It has been also determined from the numerical calculations that the neck viscosity is not very sensitive to the values of the considered packing angles.

In order to use kinetic equations (8) and (9) for the prediction of the material consolidation, the dimensionless neck radius x/R has to be related to the porosity of the material. For the considered geometry, porosity is defined as a ratio of the empty volume within the conical element to its total volume (see Fig. 1). This definition gives for the initial porosity θ_0^{45} of the simple cubic packing $\theta_0^{45} = 0.414$; and, for the initial porosity θ_0^{30} of f.c.c. packing, it gives $\theta_0^{30} = 0.196$. These porosities are slightly lower than the real porosities of these types of packing, which are equal to 0.47 and 0.26, respectively. The difference appears due to the approximated character of the axisymmetrical unit cell and it is important only for small porosity levels comparable with the error in the porosity determination.

Neck radiuses as functions of porosity for different values of ξ and $\varphi = \pi/4$ are given in Fig. 3. The curves shown in this picture consist of two parts. The first part is a non-equilibrium part sensitive to ξ value, and the second part is a quasi-equilibrium part common for all curves. As a result, two different stages in neck evolution have to be considered. During the first stage, the surface diffusion is the dominant mechanism of the neck growth, the neck rapidly increases with a small porosity change. The turning point of this process depends on the relative rates of the grain-boundary and the surface diffusions. It seems reasonable to use different approximations for the different stages of the neck evolution. For example, for $\xi = 0.1$ and $\varphi = \pi/4$

$$\begin{aligned} x/R &= 1.59\sqrt{\theta_0^{45} - \theta} + 0.37\sqrt[4]{\theta_0^{45} - \theta} && \theta_0^{45} - \theta \leqslant 0.04 \\ x/R &= 6.0(\theta_0^{45} - \theta)^3 - 3.07(\theta_0^{45} - \theta)^2 + 1.1(\theta_0^{45} - \theta) + 0.418 && \theta_0^{45} - \theta > 0.04 \end{aligned} \tag{11}$$

and for the same ξ and $\varphi = \pi/6$

$$\begin{aligned} x/R &= 1.53\sqrt{\theta_0^{30} - \theta} + 0.28\sqrt[4]{\theta_0^{30} - \theta} && \theta_0^{30} - \theta \leqslant 0.025 \\ x/R &= 25.71(\theta_0^{30} - \theta)^3 - 4.95(\theta_0^{30} - \theta)^2 + 1.02(\theta_0^{30} - \theta) + 0.321 && \theta_0^{30} - \theta > 0.025 \end{aligned} \tag{12}$$

In various investigations the correlation between the relative neck radius x/R and the relative shrinkage $(R-w)/R$ has been studied. These curves have specific features similar to the considered $x(\theta)$ curves. As an approximation, it is often assumed that the shrinkage is a quadratic function of the neck radius, for example (German, 1996)

$$\frac{R-w}{R} = 0.25(x/R)^2 \tag{13}$$

The comparison of these approximation with the numerical results for $\varphi = \pi/4$ and different ξ is given in Fig. 4. It is clear from the picture that (13) describes the first stage of the neck development for high values of $\xi > 1$.

The neck radius is not only a function of ξ and porosity but also it is a function of the level of the applied external stress at the neck. The neck radius x/R as a function of porosity for $\xi = 0.1$, $\varphi = \pi/4$ and different stress levels is given in Fig. 5. The strong resemblance between Figs. 5 and 3 gives the idea that the influence of the external stress is similar in some way to the change of ξ. In other words, for the function $x(\theta)$, an external compressive loading gives the same effect as some proportional increase of the grain-boundary diffusion coefficient. As a result, there exists the effective ξ_{eff} that completely determines the shape of the curves. As a result of an approximation of the numerical data, it was determined that

$$\xi_{\text{eff}} = \xi - \bar{\sigma}\xi^2 \tag{14}$$

where stress is taken negative for a compressive loading. Neck radii are given in Fig. 6 as porosity functions for the same ξ_{eff}. One can see that the curves are indeed located close to each other. Relationship (14) has been used in the calculations to estimate the contribution of an external stress into the neck development. The calculations demonstrate that (14) can be used as an approximation only for the compressive negative $\bar{\sigma}$.

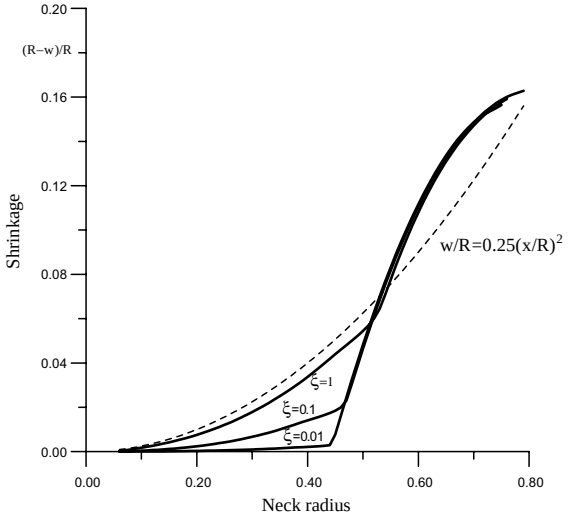

Fig. 4. Dimensionless shrinkage as a function of the neck radius for $\varphi = \pi/4$.

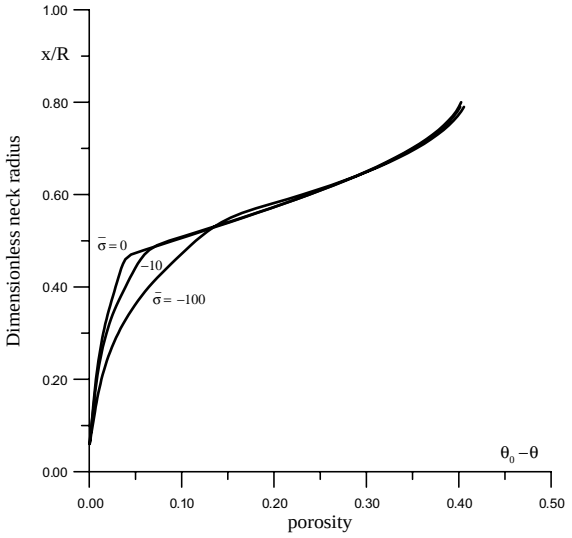

Fig. 5. Neck radius as a function of porosity for different stress levels, $\varphi = \pi/4$, $\xi = 0.1$.

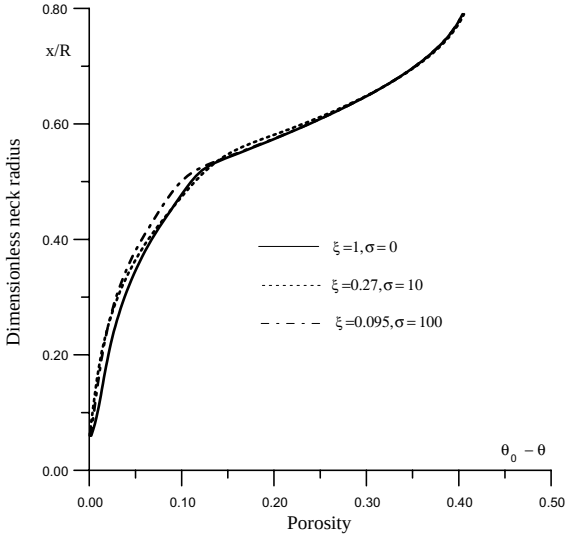

Fig. 6. Neck radius as a function of porosity for $\varphi = \pi/4$ and different combinations of the external stress and ξ with the same ξ_{eff}.

3. Modeling of deformation of agglomerated powder

As an example of the application of the obtained kinetic relationships for the description of the neck behavior during pressure-assisted sintering we consider the evolution of the density inhomogeneity in an agglomerated powder. It is assumed that a powder body consists of a mixture of powder elements with loose powder packing ($\varphi = \pi/4$) and of powder elements with an agglomerated powder ($\varphi = \pi/6$). Every powder element includes many particles. In fact, powder elements are assumed to be large enough to allow their association with some average material properties such as bulk and shear viscosities (Fig. 6).

3.1. Calculations of effective bulk viscosity of a powder body

From the rheological point of view, Eq. (9) predicts a linearly viscous behavior of the neck under loading despite the fact that particles are treated in the modeling as absolutely rigid and the viscosity of the neck is a result of the diffusion matter redistribution. The bulk viscosity of the powder compact can be estimated through the viscosities of necks and the coordination numbers. The method for the prediction of the bulk viscosity is based on the analysis of the dissipation in powder material during deformation (McMeeking and Kuhn, 1992). During sintering, the densification of a powder body takes place even without an external compressive loading. In order to describe this phenomenon the special sintering pressure P_L and the corresponding rate of the free sintering shrinkage $\dot{\varepsilon}_f$ are introduced (Rahaman, 1995). As a result, the density of the total energy dissipation in a material during sintering can be given as

$$D_{\text{total}} = (\sigma_{ij} + P_L \delta_{ij})(\dot{\varepsilon}_{ij} + \dot{\varepsilon}_f \delta_{ij}) \tag{15}$$

where σ_{ij}, $\dot{\varepsilon}_{ij}$ are stresses and strain rates in a deforming material without sintering. The sintering stress and the free sintering shrinkage rate are functions of the geometrical structure of powder compacts: particle and pores shapes, neck radiuses, particle packing. Because of the linearity of our models (Maximenko et al., 2002) they do not depend on the strain rate of a powder compact for a given geometrical structure of the compact. Hence, in the determination of the stress reaction due to the change of the strain rate during the deformation of a powder body with a given geometry, the sintering stress and the free sintering rate can be treated as constants. As a result, in the calculations of the viscosity the dissipation terms related to the sintering stress and the free sintering rate are not used, since these terms are linear with respect to the strain rates. The viscosity of a powder body is defined only by quadratic terms with respect to the strain rates (McMeeking and Kuhn, 1992). For the determination of the effective viscosity it is enough to consider only the dissipation D in the material without sintering, thereby neglecting free strain rates. The effective viscosity in the model is also a function of the geometrical structure of the material. It does not depend on the magnitude of the sintering stress or the free sintering rate. The energy dissipation D in a powder material is the sum of the energy dissipations at necks between particles, and the viscosity of a powder material can be determined through the estimations of neck viscosities.

Energy dissipation at inter-particle necks of a powder particle during deformation without sintering can be estimated as the sum of the energy dissipation of discrete necks:

$$D_1 = \frac{\pi x^2 Z}{2} \sigma \dot{w} \tag{16}$$

where coefficient 1/2 is taken due to the fact that every neck belongs to two particles. On the other hand, the energy dissipation can be estimated through the bulk viscosity K in a unit cell of the material that includes a powder particle and some empty space around it corresponding to the given porosity value (McMeeking and Kuhn, 1992):

$$D_2 = K \frac{4/3\pi R^3}{(1-\theta)} \left(3\frac{\dot{w}}{R}\right)^2 \tag{17}$$

From (16) and (17), one can obtain the following bulk viscosity:

$$K = \eta \frac{Z(x/R)^2(1-\theta)}{24} \tag{18}$$

3.2. Kinetics of densification of agglomerated powder

The linear dependence of the bulk viscosity on the coordination number in (18) shows that for the same neck size the viscosity of the agglomerates with f.c.c. packing is two times higher than the viscosity of particles in a simple cubic packing. Therefore, in general, an external pressure consolidates a simple cubic packing of particles faster than agglomerates. In principle, that could lead to the homogeneity of mesoscopic density in a powder compact. In order to check this statement at least by a first-order approximation, a self-consistent approach has been used for the assessment of the densification rate of different powder elements. The considered unit cell of the material is given in Fig. 7. The unit cell consists of a spherical powder element with some fixed coordination number of packing surrounded by an effective medium. In the theory of elastic composites self-consistent approach with the introduction of effective medium has long been in use for the assessments of elastic modulus and accumulated strains in inclusions (Aboudi, 1991). Due to the viscous-elastic analogy these results can be extended to the considered linear viscous model. Instead of strains in our case we have estimations for strain rates. The average pressure in the central powder element (see Fig. 7) can be found as a sum of the external pressure p and additional pressure p_j proportional to the difference between the average and the local densification rates (Scherer, 1984; Eshelby, 1957)

$$p_j = (e_m - e_j)\frac{4K_jG_m}{4G_m + 3K_j} \quad j = \overline{1,2} \tag{19}$$

where G_m is the average shear viscosity of the material, K_j is the local bulk viscosity, e_1 is the relative rate of volume change in the powder element with f.c.c. packing of the central spherical inclusion, e_2 is the same rate for the element with loose powder. In general, in all the relationships index 1 corresponds to the parameters of agglomerates Relationship (19) does not mean absence of shear stresses in the material. It only indicates that due to the linearity of the current problem one can consider the densification and shear effects independently. Parameter e_m is the average relative rate of the volume change and it is defined as

$$e_m = e_1 f_1 + e_2 f_2 \tag{20}$$

f_1, f_2 are volume fractions of agglomerates and loose powder, respectively.. The local e_j can be calculated as a sum

$$e_j = 3(\dot{\varepsilon}_f)_j + \frac{p + p_j}{K_j} \tag{21}$$

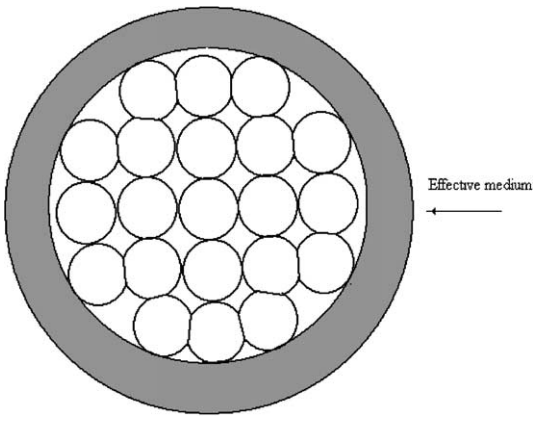

Fig. 7. Unit cell of material used for the self-consistant approach.

where p is the external macroscopic pressure. After substitution of (21) and (20) into (19) one can find unknown e_1,e_2 as functions of external loading and free sintering rates. The effective shear modulus in (19) has been estimated through Mori–Tanaka formulas (Aboudi, 1991)

$$G_m = G_1 + f_2(G_2 - G_1)G_1/((1 - f_2)(G_2 - G_1)\lambda + G_1)$$
$$\lambda = \frac{6K_1 + 2G_1}{5(3K_1 + 4G_1)} \tag{22}$$

The shear viscosities of an agglomerated and a non-agglomerated powder have been estimated through the values of bulk viscosity modules and viscous analogies of the Poisson's ratios. In the case of small non-interacting necks between particles, the viscous Poisson's ratio v_v of a powder body does not depend on the geometrical configuration of the powder packing and it is equal to 0.25 (McMeeking and Kuhn, 1992). Experimental data indicate that v_v is almost constant throughout the first stage of sintering and rapidly increases up to the incompressibility limit of 0.5 during the second stage (Du and Cocks, 1992). Using the approach proposed in (Du and Cocks, 1992) for the smooth transition of v_v from the first to the second stage, this parameter has been approximated as

$$v_v = \begin{cases} 0.25\theta \geqslant 0.07 \\ \dfrac{1 - 19.35\sqrt{\theta}(0.35 - \theta)^2}{2 + 19.35\sqrt{\theta}(0.35 - \theta)^2} \quad \theta < 0.07 \end{cases} \tag{23}$$

The plot of this function is given in Fig. 8. If current porosities are known for different types of packing, the viscous Poisson's ratios can be found from (23) and shear viscosity modulus can be estimated as

$$G_{1,2} = \frac{3K_{1,2}(1 - 2v_v)}{2(1 + v_v)} \tag{24}$$

The order of the main steps in the modeling of the isostatic densification of a powder with two types of powder packing is: (i) the assessments of the viscous parameters of the material for the given porosities,

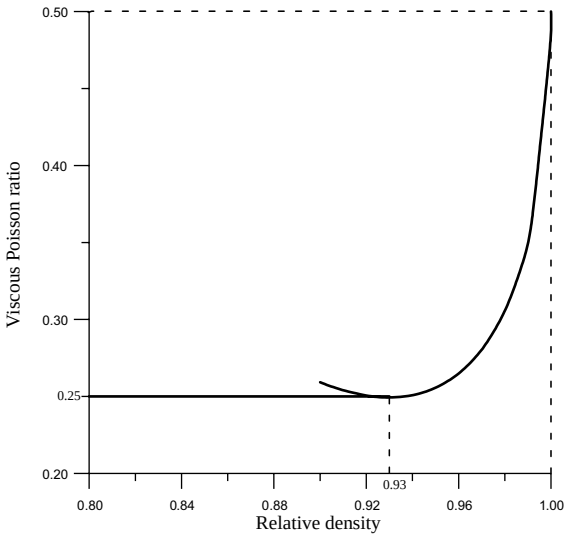

Fig. 8. Viscous Poisson's ratio as a function of the relative density.

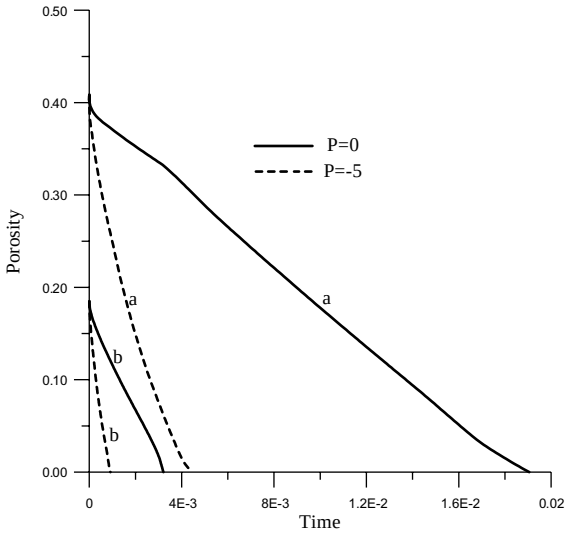

Fig. 9. Porosity evolution in agglomerates and a non-agglomerated powder for free sintering and isostatic pressure-assisted sintering: (a) porosity evolution in the elements of loose powder ($\varphi = \pi/4$); (b) porosity evolution in agglomerated powder elements ($\varphi = \pi/6$).

(ii) calculations of e_1, e_2, (iii) the prediction of the porosity change after the time increment Δt Δt based on mass conservation:

$$\Delta\theta_j = (1-\theta_j)e_j\Delta t \quad j = \overline{1,2} \tag{25}$$

Subsequently, all the procedures can be iterated through the next step.

Examples of the porosity evolution in the powder elements with loose and agglomerated powders for the volume concentration of agglomerates equal to $f_1 = 0.1$ are given in Fig. 9. During isostatic pressure-assisted sintering, the porosities of an agglomerated and a non-agglomerated powder become closer to each other. However, no external pressure can provide the homogeneous densification of a powder body. Agglomerates always reach complete density before a loose powder does. During consolidation, as a result of the applied pressure, the bulk viscosity of the non-agglomerated powder rapidly increases, since according to (18) it is proportional to the forth degree of the neck radius. Even a small change of the neck radius greatly increases the bulk viscosity of the material without a substantial change of porosity.

4. Conclusions

An axisymmetrical model of the diffusion evolution of necks between particles allows the direct calculations of the evolution of such sintering parameters as the densification rate of free sintering, the viscosity of necks between particles, the neck growth rate. The information about the neck growth rate for different packing angles and external loading levels is useful for the understanding of the densification processes in an agglomerated powder. It is shown that despite high initial viscosity of agglomerates they always reach full density before the loose powder does. This phenomenon is explained by the rapid increase of viscosity of the loose powder due to the neck growth. The isostatic pressing promotes densification but it can prevent the grain growth in dense agglomerates only through the reduction of the densification time.

Acknowledgment

The support by the NSF Divisions of Manufacturing and Industrial Innovations (Grants DMI-9985427 and DMI-0354857), Civil and Mechanical Systems (Grant CMS-0301115), and Materials Research (Grant DMR-0313346) is gratefully appreciated.

References

Aboudi, J., 1991. Mechanics of Composite Materials. Elsevier.

Allen, S.M., Thomas, E.L., 1999. The Structure of Materials. John Wiley & Sons.

Bouvard, D., McMeeking, R.M., 1996. Deformation of interparticle necks by diffusion-controlled creep. J. Am. Ceram. Soc. 79 (3), 666–672.

Du, Z.Z., Cocks, A.C.F., 1992. Constitutive model for the sintering of ceramic components—I. Material model. Acta Metall. Mater. 40 (8), 1969–1979.

Eshelby, J.D., 1957. The determination of the elastic field of an ellipsoidal inclusion and related problems. Proc. R. Soc. Lond. A 241 (1226), 376–396.

German, R.M., 1996. Sintering Theory and Practice. John Wiley & Sons.

Hague, D.C., Mayo, M.J., 1999. Sinter-forging of nanocrystalline zirconia: II, Simulation. J. Am. Ceram. Soc. 82 (3), 545–555.

Lange, F.F., 1989. Powder processing science and technology for increased reliability. J. Am. Ceram. Soc. 72 (1), 3–15.

Maximenko, A., Olevsky, E., 2004. Effective diffusion coefficients in solid-state sintering. Acta Mater. 52 (10), 2953–2963.

Maximenko, A., Roebben, G., Van Der Biest, O., 2002. Modeling of non-linear phenomena during deformation of interparticle necks by diffusion-controlled creep. Acta Mater. 50 (14), 3651–3659.

Mayo, M.J., 1995. Processing of nanocrystalline ceramics from ultrafine particles. Int. Mater. Rev. 41 (3), 81–115.

McMeeking, R.M., Kuhn, L.T., 1992. A diffusional creep law for powder compacts. Acta Mater. 40 (5), 961–969.

Rahaman, M.N., 1995. Ceramic Processing and Sintering. Marcel Dekker Inc., New York.

Scherer, G.W., 1984. Viscous sintering of a bimodal pore-size distribution. J. Am. Ceram Soc. 67 (11), 709–715.